Total attenuation compensation for backscatter coefficient estimation using full angular spatial compounding in physical phantoms

Coila, Andres, Rouyer, Julien, Zenteno, Omar, Luchies, Adam, Oelze, Michael, et al.

Andres Coila, Julien Rouyer, Omar Zenteno, Adam Luchies, Michael L. Oelze, Roberto Lavarello, "Total attenuation compensation for backscatter coefficient estimation using full angular spatial compounding in physical phantoms," Proc. SPIE 11602, Medical Imaging 2021: Ultrasonic Imaging and Tomography, 116020A (15 February 2021); doi: 10.1117/12.2580300

SPIE.

Event: SPIE Medical Imaging, 2021, Online Only

Total attenuation compensation for backscatter coefficient estimation using full angular spatial compounding in physical phantoms

Andres Coila*[a], Julien Rouyer[b], Omar Zenteno[b], Adam Luchies[a], Michael L. Oelze[a], and Roberto Lavarello[b]

[a]Beckman Institute for Advanced Science and Technology, University of Illinois at Urbana-Champaign, Urbana, Illinois, USA
[b]Laboratorio de Imágenes Médicas, Pontificia Universidad Católica del Perú, Lima, Perú

ABSTRACT

The backscatter coefficient (BSC) quantifies the frequency-dependent reflectivity of tissues. Accurate estimation of the BSC requires knowledge of the attenuation coefficient slope (ACS) of tissues in the beam path between the transducer and the insonified region of interest, namely, the total attenuation. In this study, the total attenuation is calculated as the cumulative sum of values of a local attenuation map devised using full angular spatial compounding (FASC). The BSC was parameterized through the integrated backscatter coefficient (iBSC) obtaining iBSC maps. Experimental validation of the proposed approach consisted of scanning two cylindrical physical phantoms with off-centered inclusions having different ACS and BSC values than the background. Additional iBSC maps were computed assuming an uniform ACS map of 0.5 dB/cm/MHz (which is a value assumed for soft tissues) instead of the FASC-ACS map. Finally a iBSC map was obtained using an ideal ACS map formed with ground truth ACS values and knowledge of inclusion true position. The results were comparable when using the FASC-ACS map or the ideal ACS map in term of inclusion detectability and estimation accuracy. The use of the uniform ACS map resulted in some cases with very high fractional error (>9 dB), which highlights the relevance of accurate compensation for total attenuation. These results suggest that BSCs can be reliably estimated using total attenuation compensation from FASC-ACS maps.

Keywords: backscatter coefficient, total attenuation, full angular spatial compounding, spectral-log-difference

1. INTRODUCTION

The frequency-dependent backscatter coefficient (BSC) describes how a medium reflects the incident ultrasonic energy. The BSC has shown promise for improving diagnosis of disease in the liver, lymph-nodes, thyroid, breast, among others tissues. Nevertheless, *in vivo* BSC estimation requires compensation for the ultrasonic attenuation occurring in the beam path between the transducer and the region of interest, i.e., the total attenuation. Being that the attenuation of the interrogated media is often unknown, the total attenuation compensation approaches include, for example, neglecting the impact of attenuation; simultaneous derivation of total attenuation and BSC; or cumulative sum of attenuation in the beam path based of values from the attenuation coefficient slope, e.g., a pre-selected value for soft tissues or the values from a estimated local attenuation map. The latter method is the most appropriate for providing a local attenuation map with sufficient accuracy. Moreover, in BSC estimation the full angular spatial compounding (FASC), which has potential application in breast cancer assessment given the full angular availability of this type of tissue, provides a reduction of variance in mapping the BSC in tissue-mimicking phantoms with low attenuation coefficient slope (ACS<0.1 dB/cm/MHz),[1,2] i.e., when total attenuation could be neglected. In the present work the BSC of non-negligible attenuating media is presented and estimated in a FASC setup. The total attenuation was computed using a local attenuation map derived using the FASC approach.

*Further author information: (Send correspondence to A.C.)
A.C.: E-mail: acoila@illinois.edu, Telephone: 1 217 333 1640

Medical Imaging 2021: Ultrasonic Imaging and Tomography, edited by Brett C. Byram, Nicole V. Ruiter, Proc. of SPIE Vol. 11602, 116020A · © 2021 SPIE
CCC code: 1605-7422/21/$21 · doi: 10.1117/12.2580300

2. METHODS

2.1 Ultrasonic parameters estimation

The BSC of a region of interest (ROI) can be estimated from the power spectra of gated backscattered RF echo signals within the ROI acquired with a ultrasound transducer. The frequency (f) dependent BSC of a ROI located at depth z can be obtained from the power spectrum $S(f,z)$ after compensation of effects from system/transducer $P(f)$, the beam diffraction $D(f,z)$, and the total attenuation $A(f,z)$ with

$$S(f,z) = P(f)D(f,z)A(f,z)B(f), \tag{1}$$

where $B(f)$ if the BSC. The planar reflector method by Chen et al. (Ref 3) performs a calibration of system acquisition when flat or weakly focused single-element transducers and compensation of the beam diffraction effects with analytic expressions.[3] Hence, only total attenuation remains unknown. As shown in Fig. 1, the backscattered signal from a ROI might cross several media; hence, the averaged power spectrum from an ROI can be affected by the attenuating properties of multiple layers. In the case of a soft tissue we can either assume the value 0.5 dB/cm/MHz, i.e., a uniform attenuation map or calculate the total attenuation using a estimated local attenuation map. To improve the quality of the estimated local attenuation maps the FASC[4] approach is used. Up to N acquisitions are performed and the value of a pixel is obtained after as the median value of the the single views estimates. In this work, the effects of the size of N was tested using different amount of averaging: 3, 6, 10, 15, and 30 views.

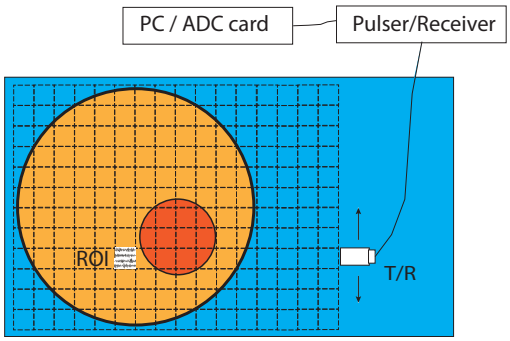

Figure 1. Diagram of acquisition of ultrasonic radio-frequency data in a water tank of a cylindrical phantom with an inclusion. For computing quantitative ultrasonic parameters of a ROI all the attenuation values of blocks between transducer and ROI are needed. A transducer in our setup was moved laterally to obtain a 2D image and the sample was rotated to obtain 360° coverage.

The total attenuation corresponding to every region of interest was computed using the FASC-ACS map obtained from N individual views. For each individual view an attenuation map was computed using the spectral-log-difference method[4,5] with $30\lambda \times 30\lambda$ data-blocks and 87.5% overlap. For comparison purposes the BSC was estimated with a pre-selected ACS map of uniform ACS=0.5 dB/cm/MHz (which is a common value used in soft tissues) and with the ideal ACS map constructed with the ground truth values and true locations of the inclusion.

2.2 Data sets

The experimental data set was obtained from two cylindrical agar-based tissue-mimicking phantoms, A and B, designed with a 7-cm diameter background with an embedded 2.5-cm diameter inclusion which had different attenuating and scattering properties than the background (attenuation and scattering controlled by different amount of graphite powder). Data acquisition was performed using a micro-positioning system with a lateral step size of 0.5 mm. A 7.5 MHz, f/4 single-element transducer driven by an Olympus Panametrics 5900 pulser/receiver (Olympus Corporation, Waltham, MA) as well as a UF3-4121 14-bit digitizer PCI-X card (Strategic Test Corporation, Woburn, MA) was used to collect the data. For this transducer, the analysis bandwidth chosen (f_L,f_H) was (4,9) MHz. The ACS ground truth values (in dB/cm/MHz) of A_{inc}, A_{bkg}, B_{inc}, B_{bkg} were 0.41, 0.75, 0.54,

and 1.04, respectively. These values were obtained from independent additional samples having the same concentration of graphite powder and scatterers and scanned using the insertion-loss method. Ground truth values of BSC were obtained with small samples using the planar reflector method[3] but using additional small samples such that the compensation of attenuation was almost negligible. The BSC was estimated with $10\lambda \times 10\lambda$ data blocks with 75% overlap.

2.3 Integrated backscatter coefficient

The integrated backscatter coefficient (iBSC) was computed as

$$\text{iBSC(x,z)} = \frac{1}{f_\text{H} - f_\text{L}} \int_{f_\text{L}}^{f_\text{H}} \text{BSC}(f,\text{x,z})\text{df}, \tag{2}$$

for every pixel located at position (x,z). Compounding of the N single views was performed in the BSCs obtained for a pixel in every available view before calculating the iBSC in equation (2). The contrast-to-noise ratio (CNR) was computed from the iBSC maps using the mean (μ) and standard deviation (σ) of the iBSC values of the inclusion and a region in the background with same size as

$$\text{CNR} = \frac{\mu_\text{inc} - \mu_\text{bkg}}{\sqrt{{\sigma_\text{inc}}^2 + {\sigma_\text{bkg}}^2}}. \tag{3}$$

The iBSC maps were further compared with the iBSC_ideal map (Fig. 2) obtained from the ground truth values of BSCs by

$$\text{AFE(x,z)}=10\log_{10}\left(\frac{\text{iBSC(x,z)}}{\text{iBSC}_\text{ideal}\text{(x,z)}}\right), \tag{4}$$

where AFE stands for absolute fractional error.

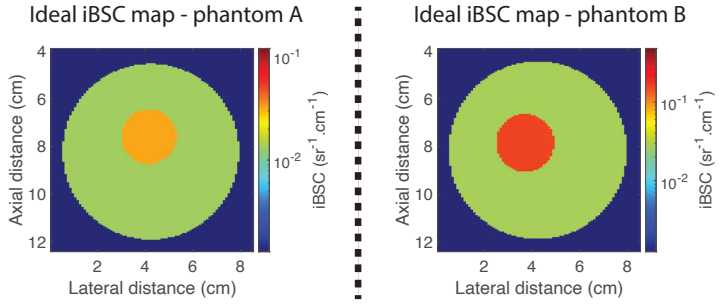

Figure 2. Ideal iBSC maps used for computing the absolute fractional error. Left: phantom A. Right: phantom B.

3. RESULTS

The attenuation maps for phantom A and B are shown are shown in Fig. 3, using RF data from a single view or multiple view. The inclusion borders are clearer when using more views in FASC. Numerically, the accuracy of values of the inclusion and background does not change dramatically; however, the standard deviation of ACS values for both inclusion and background decreases monotonically with the number of views (Fig. 4).

The iBSC maps obtained using the FASC-ACS map or a uniform ACS map for total attenuation compensation are shown in Fig. 5 and 6 for phantoms A and B, respectively. Notice that BSCs were averaged spatially with FASC approach as well depending on the number of angles (either 3, 6, 10, 15 or 30) but it can be observed that using a uniform ACS map for total attenuation compensation did not result in much improvement in the iBSC maps. However, using FASC in both the ACS maps and for BSC estimation, resulted in rapid improvement of image quality with increasing number of views.

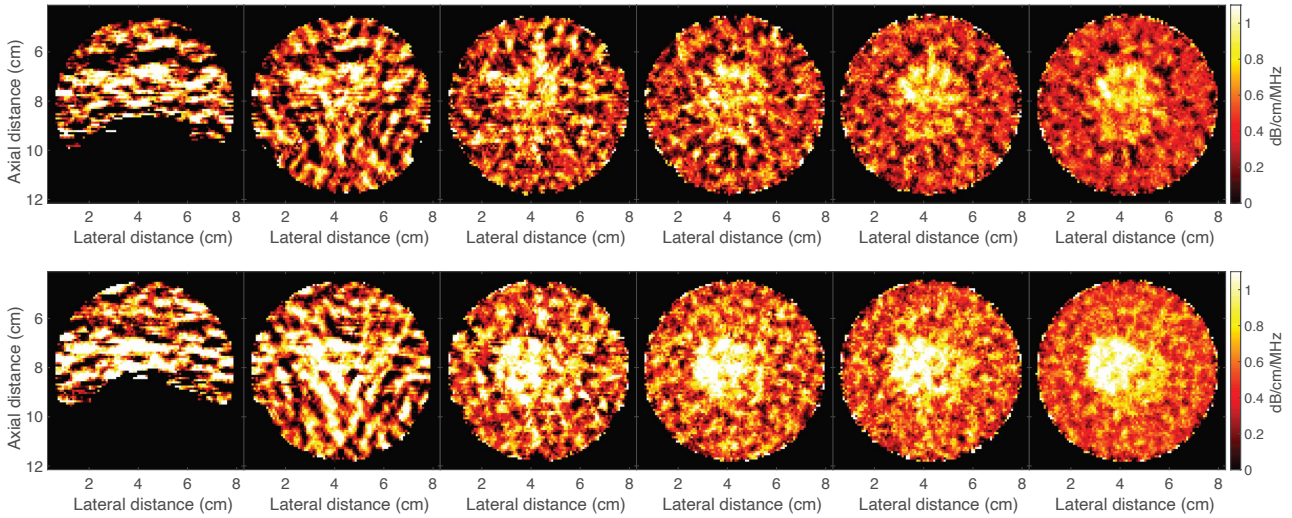

Figure 3. Attenuation images of physical phantoms A (top) and B (bottom). Starting from the left the images correspond to no compounding, and compounding of 3, 6, 10, 15, and 30 views. The increasing number of angles allow better depiction of the inclusion.

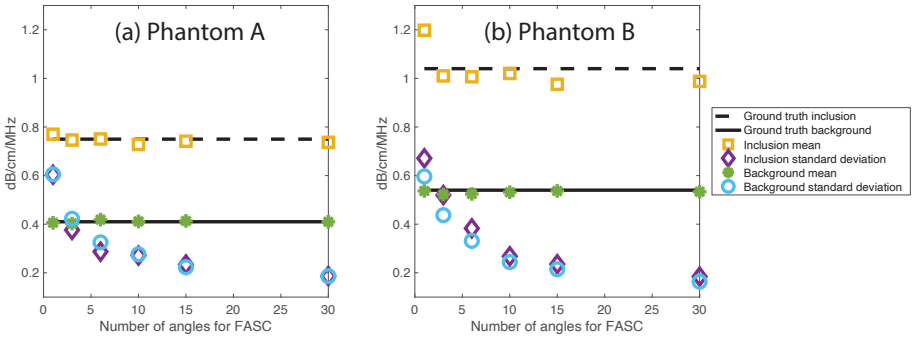

Figure 4. Mean and standard deviation of ACS of inclusion and background versus number number of angles used in FASC-ACS. The increasing number of angles mainly reduce the standard deviation within the attenuation images.

Moreover, in Fig. 6 several artifacts can be observed. First, the uniform map of 0.5 dB/cm/MHz values for compensation can produce under compensation in the inclusion of phantom B because this value is much lower than the ground truth value 1.04 dB/cm/MHz. Another advantage of FASC is that artifacts observed in single view iBSC maps at deeper regions (around 10 cm depth or more) are mitigated with the median averaging of the FASC approach.

In Fig. 7, we showed the iBSC maps constructed using an ideal ACS map and maximum spatial averaging (30 views) which resemble more to the ideal BSC maps from Fig. 2. However, in practice the perfect knowledge of local attenuation maps is not possible. Therefore, using the FASC-ACS for total attenuation compensation is the best approach.

The iBSC contrast between the inclusion and background was the lowest when using the uniform ACS map (see Fig. 8). Using the FASC-ACS map the contrast increased rapidly with the number of views N. However, using the uniform ACS map did not change drastically the CNR values vs N. For the maximum number of views, N=30, the iBSC map obtained when using the uniform ACS map (CNR=1.32) was worse than the iBSC map obtained when using the FASC-ACS map (CNR=3.05) or the ideal ACS map (CNR=4.42). Likewise, the contrast of the iBSC map when using the uniform ACS map was very low (CNR=0.132) compared to the CNR of iBSC maps obtained when using the FASC-ACS map (CNR=2.29) or the ideal ACS map (CNR=2.86).

In terms of accuracy, the mean of the fractional error for regions inside and outside the inclusion are provided in Fig. 9. In general using the FASC-ACS map or the ideal ACS map generated less fractional error, i.e., more

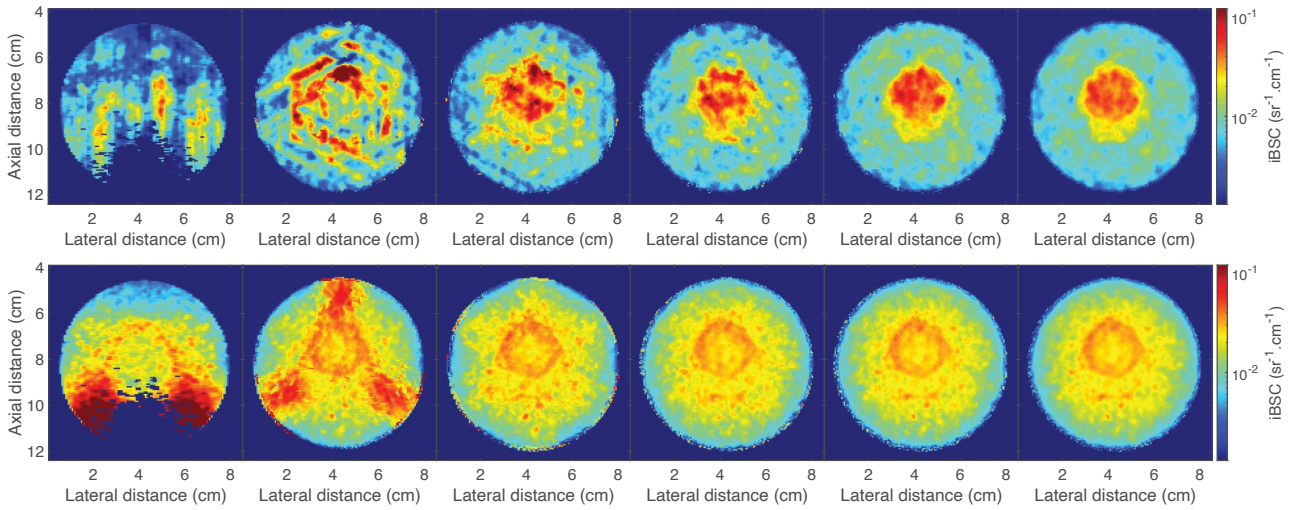

Figure 5. Top: Phantom A iBSC maps using for total attenuation FASC-ACS maps (top) or uniform ACS maps (bottom). No compounding and compounding of 3, 6, 10, 15, and 30 views are presented. Better contrast-to-noise ratio is obtained with the FASC-ACS maps (CNR=3.05 for 30 views FASC) than its uniform map counterpart (CNR=1.32).

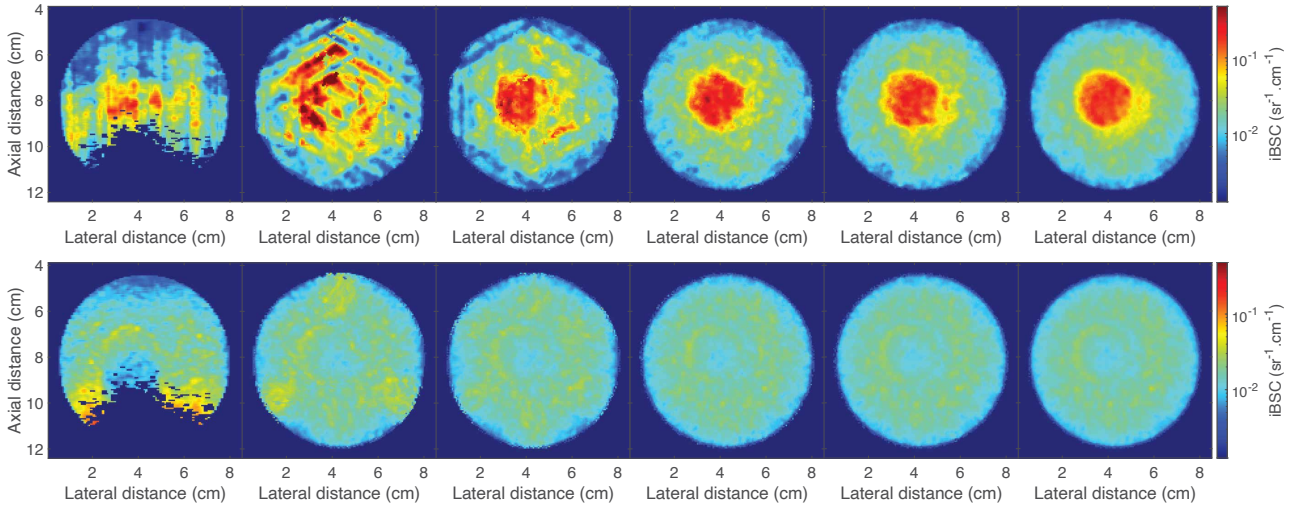

Figure 6. Top: Phantom B iBSC maps using for total attenuation FASC-ACS maps (top) or uniform ACS maps (bottom). No compounding and compounding of 3, 6, 10, 15, and 30 views are presented. Better contrast-to-noise ratio is obtained with the FASC-ACS maps (CNR=2.29 for 30 views FASC) than its uniform map counterpart (CNR=0.132).

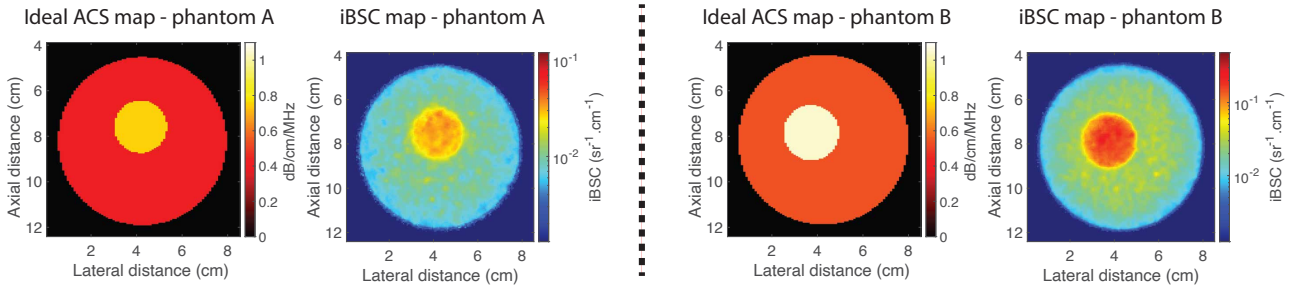

Figure 7. iBSC maps (using maximum spatial averaging of BSCs, 30) obtained using an ideal ACS map (ground truth ACS values and correct location of the inclusion). Left half: phantom A. Right half: phantom B.

accurate, except in the inclusion of phantom A. This atypical result might be explained because the data blocks within the inclusion will have had their beam path crossing mainly the background with ACS=0.41 dB/cm/MHz and partially the inclusion with ACS=0.75 dB/cm/MHz, hence the uniform value used ACS=0.5 dB/cm/MHz was relatively close to the average of these actual values.

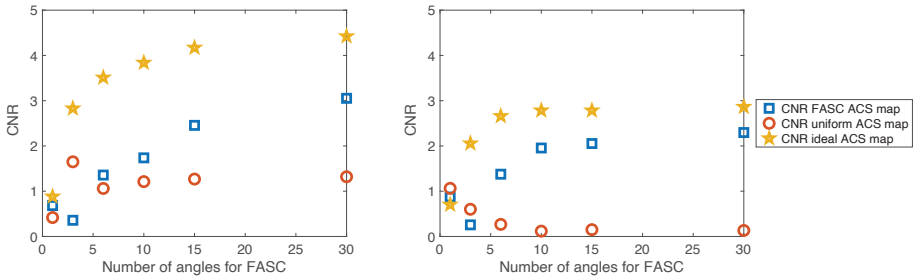

Figure 8. Contrast-to-nosie ratio of inclusion and background. The FASC-ACS map improves the CNR a factor of 2.3 for phantom A (left) and a factor of 17 for phantom B (right) with respect to the uniform map. Both approaches are mainly inferior to the use of the ideal ACS map.

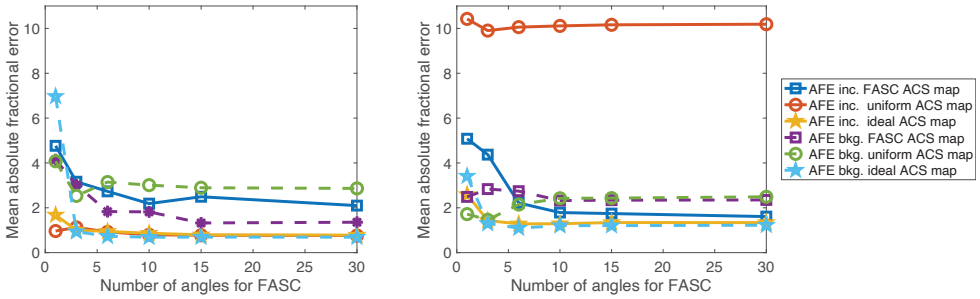

Figure 9. Mean values of absolute fractional error (AFE) in dB for the inclusion and background. The largest errors seems to occur when using the uniform ACS map; e.g., for the background of phantom A (AFE>2.5 dB) or the inclusion of phantom B (AFE>9 dB).

4. DISCUSSION AND CONCLUSION

The usefulness of the full angular spatial compounding for improved spectral-based tissue characterization was explored in this study for BSC estimation of non-negligible attenuating media.

The full angular approach resulted in accurate and precise estimates of ACS that can be effectively used for total attenuation compensation instead of using a pre-selected uniform attenuation value. Moreover, the study demonstrates that the iBSC mapping using the FASC-ACS map described most of the desired contrast of scattering properties similar to the ideal case. These results are significant because in practice the ideal ACS maps will not be available for attenuation compensation. Therefore, the use of FASC-ACS maps is an appropriate alternative. The performance obtained with this approach was comparable to the results obtained when using the actual ground truth attenuation maps and outperformed the case where iBSC was obtained using pre-selected uniform ACS maps.

ACKNOWLEDGMENTS

A. Coila acknowledges the financial support from the National Council of Science, Technology and Technological Innovation (CONCYTEC, Peru) through the National Fund for Scientific, Technological Development and Technological Innovation (FONDECYT, Peru) under grant 132-2016. This research was supported also by the 08-2013-FONDECYT grant from the Peruvian government (CONCYTEC), the DGI-2019-0693 grant from the Pontificia Universidad Catolica del Peru and the grants from the NIH (R01CA251939 and R21EB024133).

REFERENCES

[1] Lavarello, R. J., Sanchez, J. R., and Oelze, M. L., "Improving the quality of QUS imaging using full angular spatial compounding," in [*2008 IEEE International Ultrasonics Symposium (IUS)*], 32–35 (2008).

[2] Lavarello, R. J., Oelze, M. L., Berggren, M., Johnson, S., Orescanin, M., and Yapp, R., "Implementation of scatterer size imaging on an ultrasonic breast tomography scanner," in [*2009 IEEE International Ultrasonics Symposium (IUS)*], 305–308 (2008).

[3] Chen, X., Phillips, D., Schwarz, K. Q., Mottley, J. G., and Parker, K. J., "The measurement of backscatter coefficient from a broadband pulse-echo system: a new formulation," *IEEE Trans. Ultrason. Ferroelectr. Freq. Control* **44**(2), 515–525 (1997).

[4] Zenteno, O., Luchies, A., Oelze, M., and Lavarello, R., "Improving the quality of attenuation imaging using full angular spatial compounding," in [*2014 IEEE International Ultrasonics Symposium (IUS)*], 2426–2429 (2014).

[5] Labyed, Y. and Bigelow, T. A., "A theoretical comparison of attenuation measurement techniques from backscattered ultrasound echoes," *J. Acoust. Soc. Am.* **129**(4), 2316–2324 (2011).